Finite Elements in Analysis and Design 225 (2023) 104017

Contents lists available at ScienceDirect

Finite Elements in Analysis & Design

journal homepage: www.elsevier.com/locate/finel

Topology optimization for transient two-phase fluid systems with continuous behavior

Gil Ho Yoon *, Min Ku Kim

School of Mechanical Engineering, Hanyang University, Seoul, South Korea

ARTICLE INFO

Keywords:
Topology optimization
Transient two-phase fluid
Transient sensitivity analysis
Level-set method
Navier–Stokes equation

ABSTRACT

This study introduces a novel topology optimization method for transient two-phase fluid problem with continuous behavior, which remains a challenging task despite advances in computing capabilities. The application of gradient-based optimizer to continuous two-phase fluid systems is complicated because it requires some modifications of the governing equations to reflect changes in the interface between two fluids and the transient sensitivity analysis. To overcome these difficulties, this study develops a new topology optimization method for continuous two-phase fluid that models the interface using the level-set approach and formulates the transient sensitivity analysis. The study presents several optimization examples to demonstrate the validity and applicability of this approach.

1. Introduction

An extension to topology optimization method for continuous transient two-phase fluid problem is newly developed in the present study. Two-phase flow denotes a combination of two distinct phase fluids. Some typical examples are the combination of gas–liquid or liquid–liquid which can be observed in many scientific and engineering applications. For an example, Fig. 1(a) and (b) show the figures of the concept of two-phase fluid and the ink dispersion in water which require the complicated theories and simulation of the two-phase fluid. As the intricate physical phenomena between two fluids are considered, it is challenging to underline the involved physics and topologically optimize a structure for transient two-phase fluid despite increased computing capabilities. In addition, the application of a gradient based optimizer toward the two-phase fluid system is intricate as it may require the modifications of the governing equations to reflect the change of the interface between two fluids and the transient sensitivity analysis. In this study, to cope with these difficulties, a new topology optimization method for two-phase fluid is presented as shown in Fig. 1(c). The interface between two fluids is modeled with the level-set based approach and the transient sensitivity analysis is formulated. To show the validity and applicability of the present approach, several numerical examples are solved.

The large range of scientific and engineering applications for two-phase flow of immiscible fluids exist. Among others, these includes water–air sloshing in tank, cavitation, air-rising phenomenon and various microfluidic applications. Recently, the accurate numerical modeling of two-phase flow becomes challenging for the applications of polymer electrolyte membrane (PEM) fuel cell, chemical process and nuclear industry and many schemes have been developed and implemented for analysis [2–5]. In the simulation of two-phase or multiple phase fluid, the surface or interface force model is crucial and important [5]. In relevant researches with different numerical schemes for two-phase fluid, the constant surface model introduced by Brackbill for modeling surface tension is prevail and one of the troubling artifact of the CSF method is the parasitic current.

* Corresponding author.
E-mail address: ghy@hanyang.ac.kr (G.H. Yoon).

https://doi.org/10.1016/j.finel.2023.104017
Received 22 May 2023; Received in revised form 1 August 2023; Accepted 3 August 2023
Available online 17 August 2023
0168-874X/

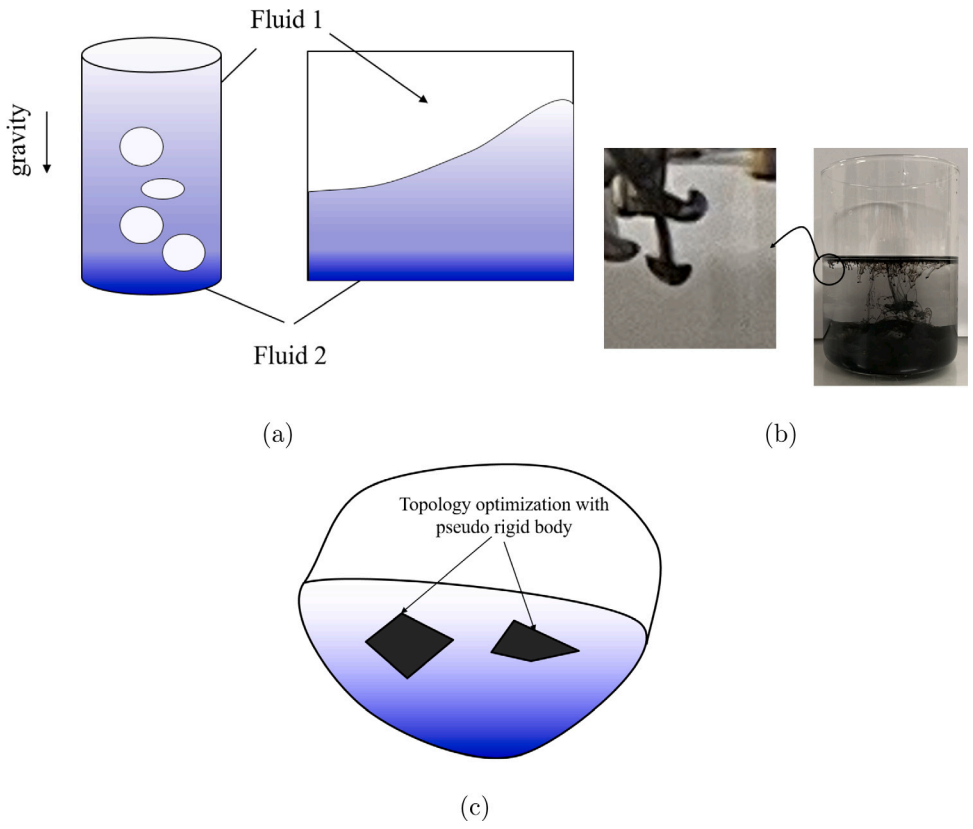

Fig. 1. Topology optimization of transient two-phase fluid. (a) Two-phase fluid examples (left: rising bubble flow, right: sloshing example), (b) Rayleigh–Taylor instability (gravity-induced shape transition in fluids [1]) and (c) the concept of topology optimization for two-phase fluid.

From a topology optimization point of view, many researches exist for fluid related problem. In [6], the Darcy force whose magnitude is proportional to the fluid velocity is added to the Navier–Stokes equation for topology optimization. With the large Darcy's force, the velocity becomes zero. Therefore, the parameterization of the Darcy's force and the optimal distribution of the Darcy's force are possible for the fluid topology optimization. Based on the concept of the novel Darcy's force, several innovative researches have been carried out [7–9]. In [10,11], the transient fluid is considered in topology optimization with the analytical sensitivity. In [12], the aerodynamic performance is optimized by topology optimization in the framework of OpenFoam. In these relevant researches, the performance of fluid is mainly considered. Then, the conjugate heat transfer system and fluid structure interaction system were considered in topology optimization. It is impossible to review and cite all relevant researches. See [13–19] and reference therein. In [13,14], the forced convection is considered in topology optimization. In [20], the natural convection is considered in topology optimization. In [21], the topology optimization with heat sink in turbulent natural convection using a RANS model is adopted. The optimized results are analyzed from a theoretical point of view using the representative number, i.e. Reynolds number and Grashof number. In [22], the TOBS method is developed for turbulent flow. Researches can be found with a variety of strategies for simultaneously considering geometric performance and manufacturability [23]. The topology optimization with two fluid heat exchange is performed in [24] which considers the separated fluids between pseudo rigid domain. In addition to these, researchers have developed a variety of strategies for simultaneously considering various physics and performances. Compared with the many structural problems (compliance minimization problem or compliant mechanism problem), few researches optimizing the usage of two-phase fluid exist.

This study presents a topology optimization scheme for transient two-phase fluid with continuous behavior. The Navier–Stokes equation with the level-set function is coupled with the VOF (Volume Of Fluid) method. In the Navier–Stokes equation, the Darcy force is then assigned for the modeling of pseudo-rigid domain for topology optimization. In the pseudo-rigid domain with a larger Darcy force, the fluid velocities becomes near zeros. The phase change in the level-set function is not allowed in the pseudo-rigid domain as the convective term, $\mathbf{u}\nabla\phi$, in the pseudo-rigid domain becomes zero or almost zero too. With the developed approach, a gradient-based optimizer can be successfully incorporated. To prove the concept of the fluid topology optimization of two-phase fluid, several examples including dam-break example and Rayleigh–Taylor's instability are considered. The effect of the mass constraint is also investigated.

The remainder of this paper is organized as follows. Section 2 provides the mathematical formula pertaining to the two-phase analysis and the development of the sensitivity analysis. Several topology optimization examples for two-phase fluid are presented in Section 3. Section 4 presents the conclusions of the study and provides suggestions for future research.

2. Topology optimization formulation for two-phase fluid

Many innovative approaches exist for the simulating steady-state or transient two-phase incompressible fluid flow with surface tension [2–5]. One of the main difficulties for the numerical simulation of surface tension dominated flow is the representation of the strong pressure discontinuity across the interface boundary between multiple fluids. In addition, the accurate representation of the interface boundary is one of the important factors to describe the evolution of the interface boundary. Several moving mesh algorithms with moving mesh exist for the numerical simulation of two-phase fluid [25,26]. This aspect becomes challenges in connection to the topology optimization with fixed mesh for two-phase fluid. To address this aspect, this research employs the level-set based modeling with the surface tension modeling [2–5]. As it is complicate to consider complex interface with the level-set method, this research limits simpler boundary shapes in the considered optimization problems.

2.1. Two-phase fluid simulation

Complying with the continuum condition, the transient fluid flow is governed by the momentum conservation equation with the gravity force, $\rho\mathbf{g}$, and the surface tension force, $\mathbf{F}_{\mathrm{st}}$.

$$\rho\frac{\partial\mathbf{u}}{\partial t}+\rho(\mathbf{u}\cdot\nabla)\mathbf{u}=-\nabla p+\mu\nabla\cdot\left(\nabla\mathbf{u}+\nabla\mathbf{u}^{\mathrm{T}}\right)\cdot\mathbf{u}+\rho\mathbf{g}+\mathbf{F}_{\mathrm{st}},\mathbf{u}=\mathbf{u}(\mathbf{x},t) \tag{1}$$

The velocities and pressure of fluid are denoted by $\mathbf{u}$ and p, respectively. The coordinate of a material point is denoted by $\mathbf{x}$ and the time is denoted by t. The viscosity and the density are denoted by μ and ρ, respectively. The gravity constant in vector form is given as $\mathbf{g}$ and the surface tension force which can be formulated as the body force is denoted by $\mathbf{F}_{\mathrm{st}}$. This force is defined along the interface boundary Γ. In the simulation of two-phase fluid, the formulation and numerical simulation of the surface tension force differ from that of one-phase fluid simulation. The mass conservation equation is defined as follows:

$$\frac{\partial\rho}{\partial x}+\nabla\cdot(\rho\mathbf{u})=0 \tag{2}$$

$$\text{In case of incompressible homogeneous fluid: } \nabla\cdot\mathbf{u}=0 \tag{3}$$

The above equations are subject to the initial conditions $\mathbf{u}|_{t=0}=\mathbf{u}_0$ where the initial velocity is denoted by $\mathbf{u}_0$. The boundary conditions are set as follows:

$$\begin{aligned}&\text{No}-\text{slip b.c.}:\mathbf{u}=\mathbf{0}\text{ on }\Gamma_{u^0}\\&\text{Inflow/outflow b.c.}:\mathbf{u}=\mathbf{u}^*\text{ on }\Gamma_{u^*}\\&\text{Pressure b.c.}:\left[-p\mathbf{I}+\mu(\nabla\mathbf{u}+\nabla\mathbf{u}^{\mathrm{T}})\right]\cdot\mathbf{n}=p_p\mathbf{n}\text{ on }\Gamma_{p^*}\end{aligned} \tag{4}$$

The no-slip boundary condition is defined along Γ_{u^0}, and the inflow/outflow boundary condition is defined as $\mathbf{u}^*$ along the Γ_{u^*}. Along Γ_{p^*}, the pressure boundary condition is imposed. The normal vector along the boundary is denoted by $\mathbf{n}$.

In order to take it to account the evolution of two-phase fluid within fixed Eulerian mesh, the level-set (or the phase field) based approach can be employed. By employing the continuous function ϕ, the domains of two fluids as well as the interface boundary can be determined as follows:

$$\phi(\mathbf{x},t)=\begin{cases}0 & \text{if }\mathbf{x}\in\text{Fluid 1}\\ \text{Otherwise} & \text{if }\mathbf{x}\in\text{Interface boundary }\Gamma\\ 1 & \text{if }\mathbf{x}\in\text{Fluid 2}\end{cases} \tag{5}$$

where the interface boundary condition is defined by Γ inside the analysis domain. The original level-set variable determines the kind of fluid and the interface boundary with the following equation.

$$\frac{\partial\phi}{\partial t}+\mathbf{u}\cdot\nabla\phi=0 \tag{6}$$

To improve the convergence and impose the regulation, it is known that the re-initialization process is necessary [27]. In the present study, the following modification on the level-set function is made with the reinitialization factor [28].

$$\frac{\partial\phi}{\partial t}+\mathbf{u}\cdot\nabla\phi-\gamma_L\nabla\cdot\left(\varepsilon\nabla\phi+\phi(1-\phi)\frac{\nabla\phi}{|\nabla\phi|}\right)=0 \tag{7}$$

where the parameter for interface thickness is denoted by ε and the re-initialization parameter is denoted by γ_L. With this approach, the breakup or coalescence of bubble and droplet can be simulated as the level-set value can be merged or separated. The no-flow boundary condition is defined as follows:

$$\mathbf{n}\cdot\left(\mathbf{u}\phi-\gamma_L\varepsilon\nabla\phi+\gamma_L\phi(1-\phi)\frac{\nabla\phi}{|\nabla\phi|}\right)=0 \tag{8}$$

Being dealing with flow with more than one fluid, it is necessary to take the surface tension along the fluid interface into account. The calculation of the free surface profile between fluids is a key factor in the accurate simulation of two-phase fluid. The surface tension can be modeled as a body force defined along the interface by employing the Continuum Surface Force model [5,29]. With the above level-set parameter, it is possible to define the surface tension force, $\mathbf{F}_{\mathrm{st}}$, as follows:

$$\mathbf{F}_{\mathrm{st}}=\nabla\cdot[\sigma(\mathbf{I}-\mathbf{n}_{\mathrm{int}}\mathbf{n}_{\mathrm{int}}^{\mathrm{T}})\delta_{\mathrm{int}}] \tag{9}$$

where the normal direction vector of the interface boundary is $\mathbf{n}_{\text{int}} = \frac{\nabla\phi}{|\nabla\phi|}$ and δ_{int} is defined as $6\,|\phi(1-\phi)|\,|\nabla\phi|$. The surface tension coefficient is denoted by σ. The density and the viscosity are then interpolated with respect to the normalized level-set variable, ϕ_{n}.

$$\phi_{\text{n}} = \min(\max(\phi, 0), 1) \tag{10}$$

$$\rho = \rho_1 + (\rho_2 - \rho_1)\phi_{\text{n}} \tag{11}$$

$$\mu = \mu_1 + (\mu_2 - \mu_1)\phi_{\text{n}} \tag{12}$$

where the density values of the first fluid and the second fluid are ρ_1 and ρ_2, respectively. The viscosity values of the first fluid and the second fluid are μ_1 and μ_2, respectively. The above equations are able to be solved with the finite element procedure. During the simulation, it is challenging to capture the pressure difference and track the evolution of the interface boundary condition stably. As the fluid velocity is different depending on the kind of fluid, the CFL number (Courant–Friedrichs–Lewy Number, $u\frac{\Delta t}{\Delta x}$ with u for fluid velocity, Δt for time step, and Δx for mesh size) is one of the parameters in the simulation [30]. In this study, the maximum CFL value is limited less than 0.5.

2.2. Topology optimization formulation for two-phase fluid

The purpose of the fluid topology optimization is to design pseudo rigid domain in two-phase fluid to optimize or modify fluid motion as intended. For topology optimization, the above equations should be modified in order to take it to account the change of the design variable. As the level-set variable determines the kind of fluid, it is necessary to introduce another state in topology optimization.

To model the pseudo rigid domain in the Navier–Stokes equation, the Darcy's force, $-\alpha\mathbf{u}$, is added into the moment equation. The α term is spatially varied with respect to the design variable, γ, as follows:

$$\alpha = \alpha^F_{\max}\gamma^n \tag{13}$$

where the maximum Darcy's force is denoted by $\alpha^F_{\max}$ and the spatial design variables are denoted by γ and the penalization of the SIMP method is n. The fluid equation is modified by adding this force term.

$$\rho\frac{\partial\mathbf{u}}{\partial t} + \rho(\mathbf{u}\cdot\nabla)\mathbf{u} = -\nabla p + \mu\nabla\cdot\left(\nabla\mathbf{u} + \nabla\mathbf{u}^{\text{T}}\right)\cdot\mathbf{u} + \rho\mathbf{g} + \mathbf{F}_{\text{st}} - \alpha\mathbf{u} \tag{14}$$

$$-\nabla\cdot\mathbf{u} = 0 \tag{15}$$

It is also necessary to consider the necessity of the modification of the properties of the level-set equation or the transportation equation. Here note that the value of ϕ is set to arbitrary value when $\gamma = 1$ to represent the rigid domain. It is noticed that the fluid velocity basically determines the evolution of the level-set function, i.e., $\mathbf{u}\cdot\nabla\phi$. Therefore, the fluid penalization can be sufficient to model the rigid domain in the level-set approach. However, to improve the convergence, it is also possible to modify the level-set equation.

We should emphasize that in principle, the two-phase fluid can be analyzed but, this approach and the above modifications can cause some numerical unconvergence and error in the VOF method. To our best knowledge, the numerical errors of the VOF approach are unavoidable when the distance of interface is on the order of a few grid cells due to the spurious modes. Thus, it is intricate to determine whether such evolution are physical or due to this numerical error. As the numerical error can be significant with the above artifact modification, this research chooses the numerical examples without separation or significant evolution.

For the topology optimization, the transient sensitivity analysis should be calculated. For the present study, the objective function, J, is defined as follows:

$$J(\mathbf{u}, \nabla\mathbf{u}, \phi; \gamma) = \int_{\Omega_0} f(\mathbf{u}, \nabla\mathbf{u}, \phi; \gamma)d\Omega\Big|_{t=t_f} \tag{16}$$

where the final simulation time is t_f and the objective function is defined as the integration of a function f defined at the analysis domain Ω_0. The Lagrange function, $\mathcal{L}$, then can be defined with the Lagrange multipliers, $\mathbf{u}^a, p^a, \phi^a$, as follows:

$$\begin{aligned}\mathcal{L}(\mathbf{u}, p, \gamma) &= J(\mathbf{u}, \nabla\mathbf{u}, \phi; \gamma)\\ &+ \int_0^{t_f}\int_{\Omega_0}(\mathbf{u}^a, p^a, \phi^a)\mathbf{EQ}(\mathbf{u}, \nabla\mathbf{u}, p, \nabla p, \phi, \nabla\phi, \gamma)d\Omega dt\end{aligned} \tag{17}$$

where the column set of monolithic equations for the fluid and solid is denoted by $\mathbf{EQ}$. The objective function is denoted as $J(\mathbf{u}, \nabla\mathbf{u}, \phi; \gamma)$. The calculus of variation is applied as follows:

$$\delta\mathcal{L} = \mathbf{0} \tag{18}$$

$$\begin{aligned}\delta\mathcal{L} =& \frac{\partial\mathcal{L}}{\partial\mathbf{u}}\cdot\delta\mathbf{u} + \frac{\partial\mathcal{L}}{\partial\nabla\mathbf{u}} : \nabla\delta\mathbf{u} + \frac{\partial\mathcal{L}}{\partial p}\cdot\delta p + \frac{\partial\mathcal{L}}{\partial\nabla p} : \nabla\delta p\\ &+ \frac{\partial\mathcal{L}}{\partial\phi}\cdot\delta\phi + \frac{\partial\mathcal{L}}{\partial\nabla\phi} : \nabla\delta\phi + \frac{\partial\mathcal{L}}{\partial\gamma}\cdot\delta\gamma = \mathbf{0}\end{aligned} \tag{19}$$

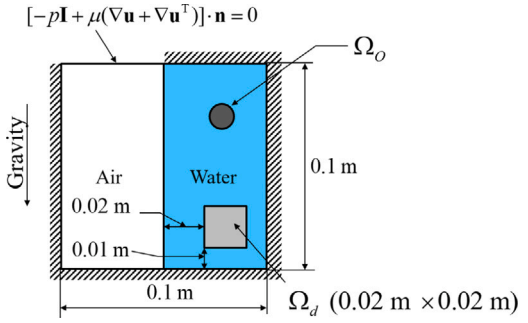

Fig. 2. Separated fluid example ($\gamma_L = 1$, $\epsilon_{ls} = 0.001$, mesh = 100 by 100, fluid: $\rho_2 = 997.92$ kg/m^3, $\mu_2 = 10^{-3}$ kg/ms, air: $\rho_1 = 1.3387$ kg/m^3, $\mu_1 = 1.8140^{-5}$ kg/ms, simulation time: 0.03 s, Incremental time (dt) = 0.001 s, $n = 3$, $\sigma = 0.07269$ N/m, Objective domain: Ω_O).

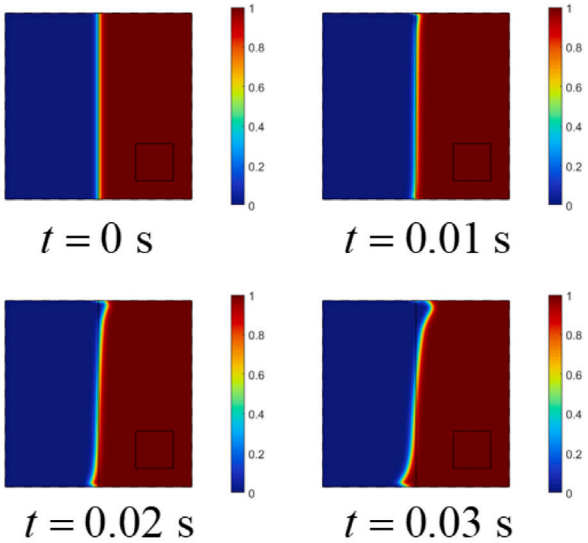

(a)

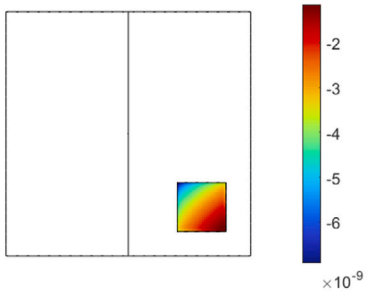

Position	FDM	Adjoint	Difference (%)
(0.0705,0.0105)	-3.4347E-09	-3.5052E-09	2.011
(0.0855,0.0105)	-1.4803E-09	-1.4533E-09	1.858
(0.0895,0.0215)	-2.1836E-09	-2.2153E-09	1.431
(0.0755,0.0115)	-2.6576E-09	-2.5454E-09	4.408
(0.0795,0.0115)	-2.1736E-09	-2.0126E-09	8.000
(0.0795,0.0145)	-2.3385E-09	-2.2275E-09	4.983
(0.0845,0.0115)	-1.5570E-09	-1.4396E-09	8.155
(0.0855,0.0125)	-1.4579E-09	-1.4314E-09	1.851
(0.0825,0.0175)	-2.2600E-09	-2.2155E-09	2.009
(0.0795,0.0225)	-3.3844E-09	-3.2406E-09	4.437
(0.0805,0.0235)	-3.3445E-09	-3.2656E-09	2.416
(0.0855,0.0205)	-2.3522E-09	-2.3118E-09	1.748
(0.0855,0.0235)	-2.7248E-09	-2.6671E-09	2.163
(0.0855,0.0285)	-3.4517E-09	-3.5662E-09	3.211

(b)

Fig. 3. Sensitivity analysis example (Objective: $\int_{\Omega_0} |\mathbf{u}|\, d\Omega|_{t=t_f}$, Ω_0: a circle with 0.01 m radius centered at (0.08 m, 0.08 m)).

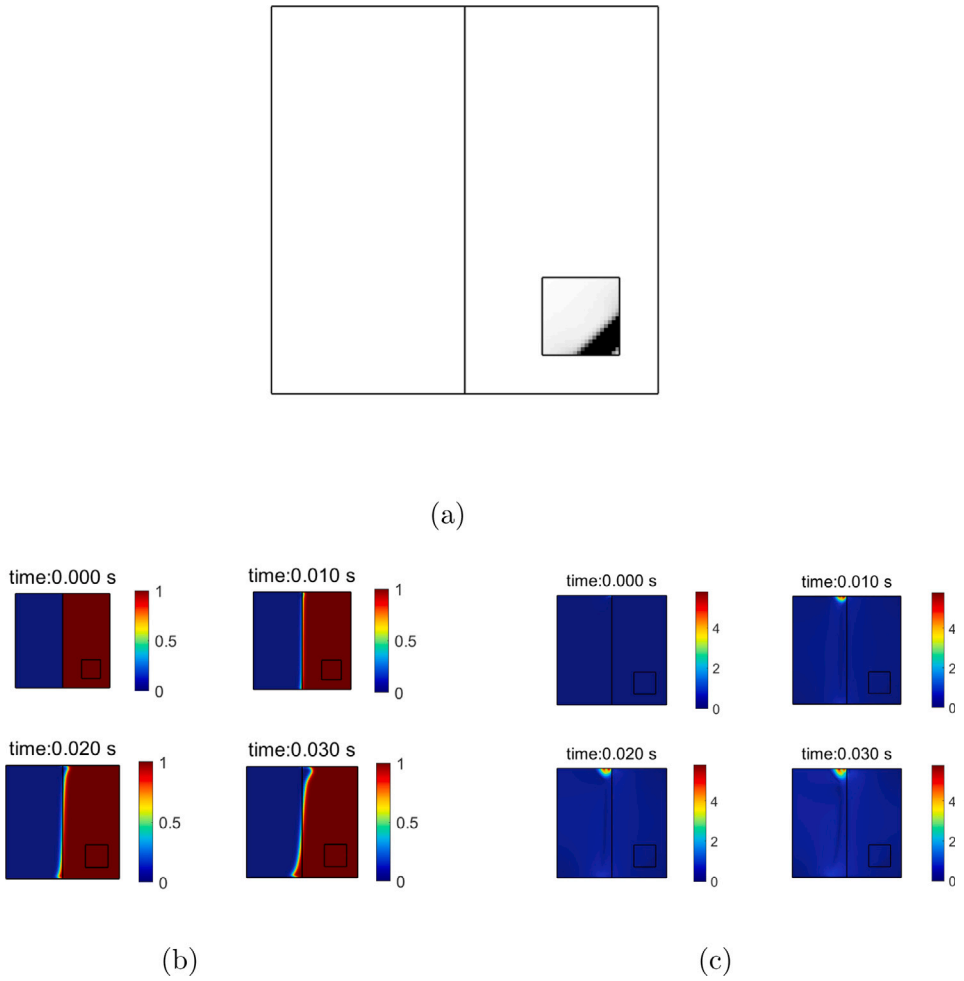

Fig. 4. Vertical two-phase problem (30 percent mass constraint, Objective: 6.9383×10^{-6} m^3/s, void design 7.0252×10^{-6} m^3/s, solid design : 6.0543×10^{-6} m^3/s). (a) The optimized layout, (b) the evolution of phase and (c) the fluid velocity.

The adjoint equations can be derived by setting the terms associated with the primal variables to zeros and with proper boundary conditions (see [31] and references therein) as follows:

$$\frac{\partial \mathcal{L}}{\partial \mathbf{u}} \cdot \delta \mathbf{u} + \frac{\partial \mathcal{L}}{\partial \nabla \mathbf{u}} : \nabla \delta \mathbf{u} = \mathbf{0} \tag{20}$$

$$\frac{\partial \mathcal{L}}{\partial p} \cdot \delta p + \frac{\partial \mathcal{L}}{\partial \nabla p} : \nabla \delta p = \mathbf{0} \tag{21}$$

$$\frac{\partial \mathcal{L}}{\partial \phi} \cdot \delta \phi + \frac{\partial \mathcal{L}}{\partial \nabla \phi} : \nabla \delta \phi = \mathbf{0} \tag{22}$$

The final sensitivity is shorten as the last term of the equation of (19) and the term of the dependency of the porosity term in the Navier–Stokes equation appears. To numerically test the above implementation, the analysis problem in Fig. 2 is considered. The right half side is filled with water and the left side is filled with air. Due to the gravity, the water eventually drops and fills the left side. For topology optimization, an optimized layout at the design domain Ω_d is pursuit to maximize the norm of the fluid velocity in the objective domain, Ω_0. The simulation time is set to 0.03 s. The phase change and the sensitivity analysis are presented in Fig. 3. As shown, it is possible to simulate the fluid drop and obtain the accurate sensitivity. In our simulation, the Newton–Raphson solver and the BDF time-dependent solver are employed. The sensitivity analysis assumes that the residual of the nonlinear equation is set to zero but in the numerical simulation, some tolerances exist.

3. Optimization examples

Several structures are topologically optimized in this section. The elucidated monolithic design approach for two-phase fluid system is analyzed utilizing the finite element method. Subsequent to obtaining the primary variables, the adjoint equations are

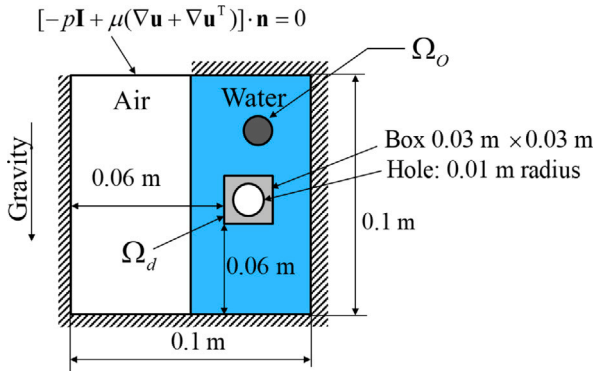

Fig. 5. Problem definition with a circle hole (γ_L = 1, ϵ_{ls} = 0.001, mesh = 100 by 100, fluid: ρ_2 = 997.92 kg/m^3, μ_2 = 10^{-3} kg/ms, air: ρ_1 = 1.3387 kg/m^3, μ_1 = 1.8140^{-5} kg/ms, simulation time: 0.03 s, Incremental time (dt) = 0.001 s, n = 3).

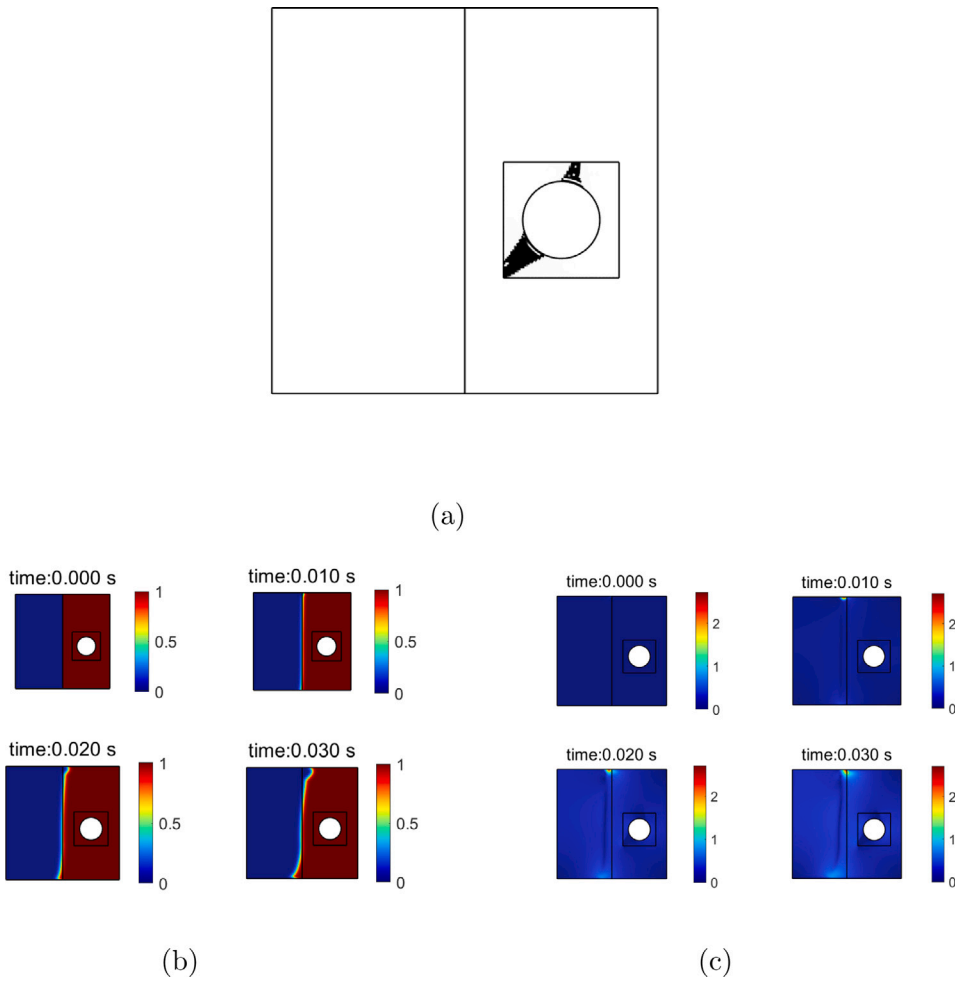

Fig. 6. Vertical two-phase problem with a hole (a) The optimized layout (Objective: 5.8451 × 10^{-6} m^3/s, solid design: 3.0672 × 10^{-6} m^3/s, void design: 5.5601 × 10^{-6} m^3/s), (b) the evolution of phase and (c) the fluid velocity.

solved to determine the sensitivity values. The calculated sensitivity values are then employed to update the design variables using the method of moving asymptotes (MMA) [32]. For the convergence, the optimization algorithm is terminated when the convergence of the objective function falls below a specified threshold within one hundred iterations.

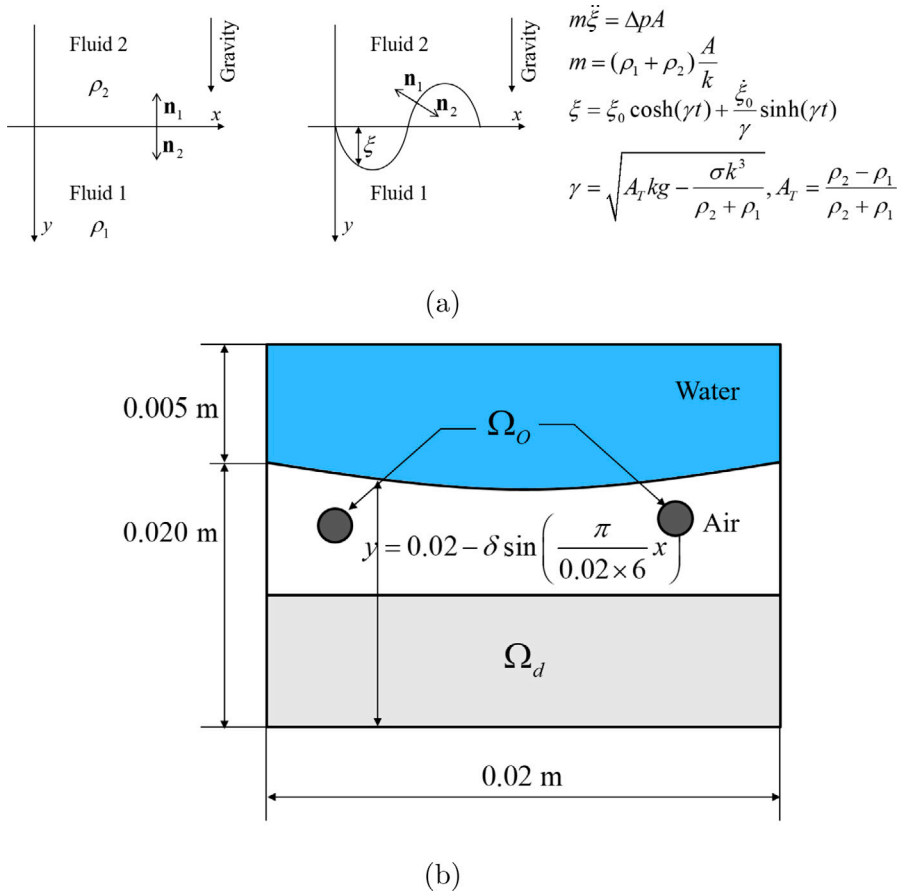

Fig. 7. Rayleigh–Taylor instability. (a) The linearized solution of Rayleigh–Taylor instability (μ_1 = 1.8140 × 10^{-5} Pa s μ_2 = 10^{-3} Pa s, ρ_1 = 1.3387 Pa s kg/m^3, ρ_2 = 997.92 kg/m^3, σ = 0.07 N/m, g = 9.81 m/s^2, $k = \pi/2/0.02$, δ = 0.001 m, Simulation time: 0.1 s, time increment = 4 × 10^{-4} s), and (b) the definition of optimization problem.

3.1. Example 1: vertically separated two-phase fluid problem

For the first optimization example, the situation with initially separated two-phase fluid is considered in Fig. 3. Due to the gravity, the fluid initially located at the right side drops. A rectangular design domain is posed in the middle of the analysis domain. The following optimization formulation is set with the norm of the fluid velocity as the objective function.

$$\begin{aligned} &\underset{\gamma}{\text{Min}} \quad J = -\int_{0_\Omega} |\mathbf{u}|_{t=t_f} \mathrm{d}\Omega \\ &\text{Subject to} \sum_{e=1}^{N_e} \gamma_e \mathrm{v}_e \geq \text{mass}_0 \\ &\gamma = [\gamma_1, \gamma_2, \ldots, \gamma_{N_e}], \quad \gamma_{\min} \leqslant \gamma \leqslant 1, \quad \gamma_{\min} = 0.001 \end{aligned} \tag{23}$$

Note that the norm of the velocity at the circular shaped target domain is set to the objective value with the mass constraint. By solving this optimization problem, one may anticipate an optimized layout with leading a notable reduction in resistance encountered during flow. The volume and the design variable of the eth element are denoted by v_e and γ_e, respectively. The total number of the design variables is denoted by N_e and the allowable mass is denoted by mass_0. The lower bound of the design variable is denoted by $\gamma_{\min}$. It can be postulated that no-structure or void structure without any blocking force can be one of possible optimal designs. Therefore, not presented here but the less than constraint provides the void design maximizing the velocity at the objective domain. Therefore, rather than imposing a less-than mass constraint, a larger-than mass constraint is imposed in this research. In some relevant studies, the resistance Darcy force is modeled as a monotonically decreasing function, and a monotonically decreasing mass constraint is imposed for fluid-related topology optimization. However, this research adopts the SIMP function, which is monotonically increasing with respect to the design variable. In short, to obtain a meaningful design, the objective is to maximize the fluid velocity subject to the "larger than or equal to" mass constraint in the objective domain. Fig. 4(a) illustrates the optimized layout, while Fig. 4(b) and (c) depict the evolution plots of the phase change and fluid velocity, respectively. Owing to

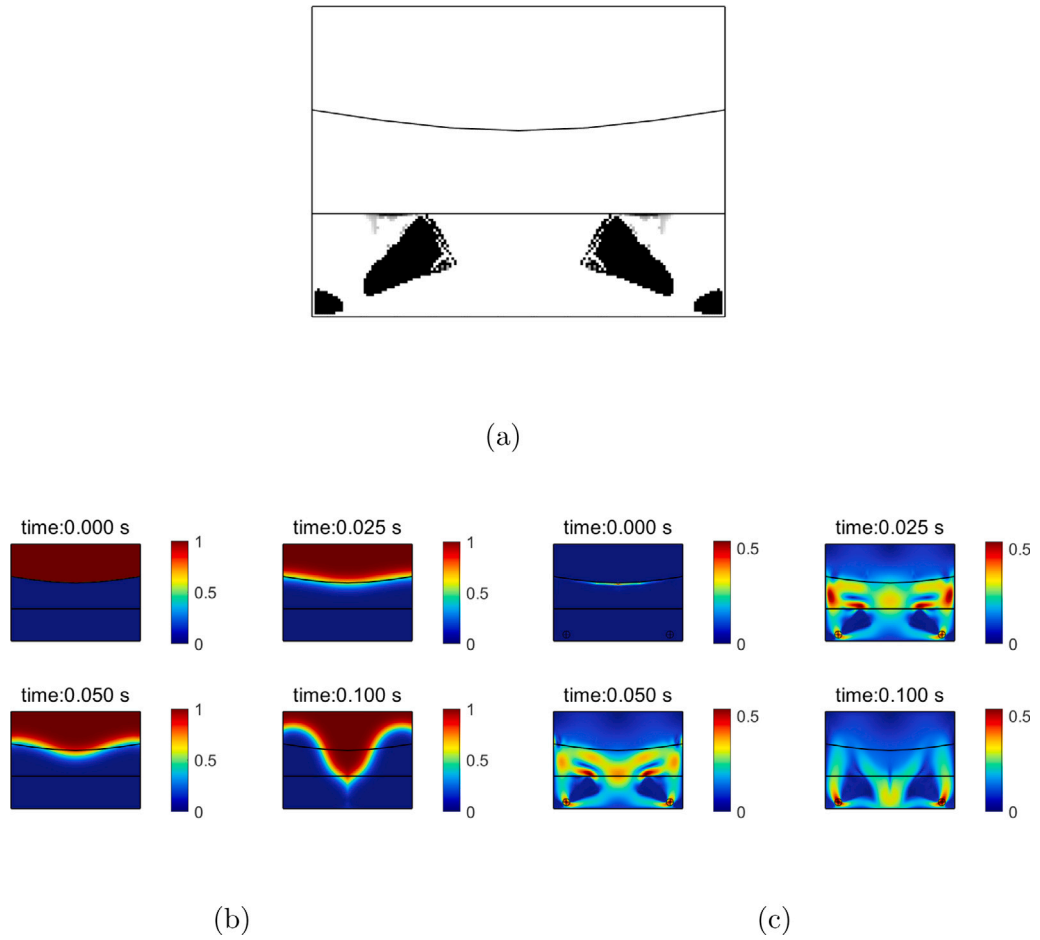

Fig. 8. (a) An optimized result ($x_1 = 0.002$ m, $x_2 = 0.008$ m, $y_1 = y_2 = 0.011$ m, $\sigma = 2.5 \times 10^{-4}$ N/m), (b) and (c) the phase plot and the corresponding fluid velocity.

the gravitational force, water initially located within the objective domain descends, and the structure in the inclined design domain redirects the fluid velocity, resulting in an enhanced objective function, namely the fluid velocity at the objective domain. In addition, a comparison of the objective functions of the void structure, the solid structure, and the optimized layout is presented. From a critical standpoint, there are some limitations to address in this study concerning the optimization process. One major constraint lies in the potential abrupt and substantial changes that can occur in the objective function due to the significant variations in fluid velocity and phase; for an example, when fluid hits the right wall, some droplets can be generated and merged. These alterations cannot be adequately accounted for using the gradient-based optimization method. It is essential to emphasize that the simulation of the two-phase fluid does accommodate these significant and non-differentiable variations. For instance, in this example, when the fluid collides with the wall, water will separate and merge over time. The current state-of-the-art simulation technique aims to capture these phenomena qualitatively rather than quantitatively. As a result, conducting topology optimization based on such stochastic and qualitative analyses may encounter convergence issue.

As an extension of the first example, the circle hole is posed in the middle of the right domain as shown in Fig. 5. By posing the circle hole, the water movement is inherently resisted. Therefore, the objective domain is partially blocked and the purpose of this optimization problem is to design the rim of the circle hole to maximize the objective function or the fluid velocity. Fig. 6(a) shows an optimized layout with the above optimization formulation. The upper and the bottom structures appear to guide the fluid motion or maximize the fluid velocity. Fig. 6(b) and (c) show the phase change and the fluid motions as time goes by. This example demonstrates that the proposed scheme can be employed to control fluid motion, and the mass constraint should be determined based on the characteristics of the optimization problem under consideration.

3.2. Example 2: Maximizing fluid velocity considering Rayleigh–Taylor instability

For the next example, this subsection considers the topology optimization maximizing the norm of fluid induced by the Rayleigh–Taylor instability [1]. The Rayleigh–Taylor instability is observed between multiple fluids of different densities as shown in Figs. 1(b)

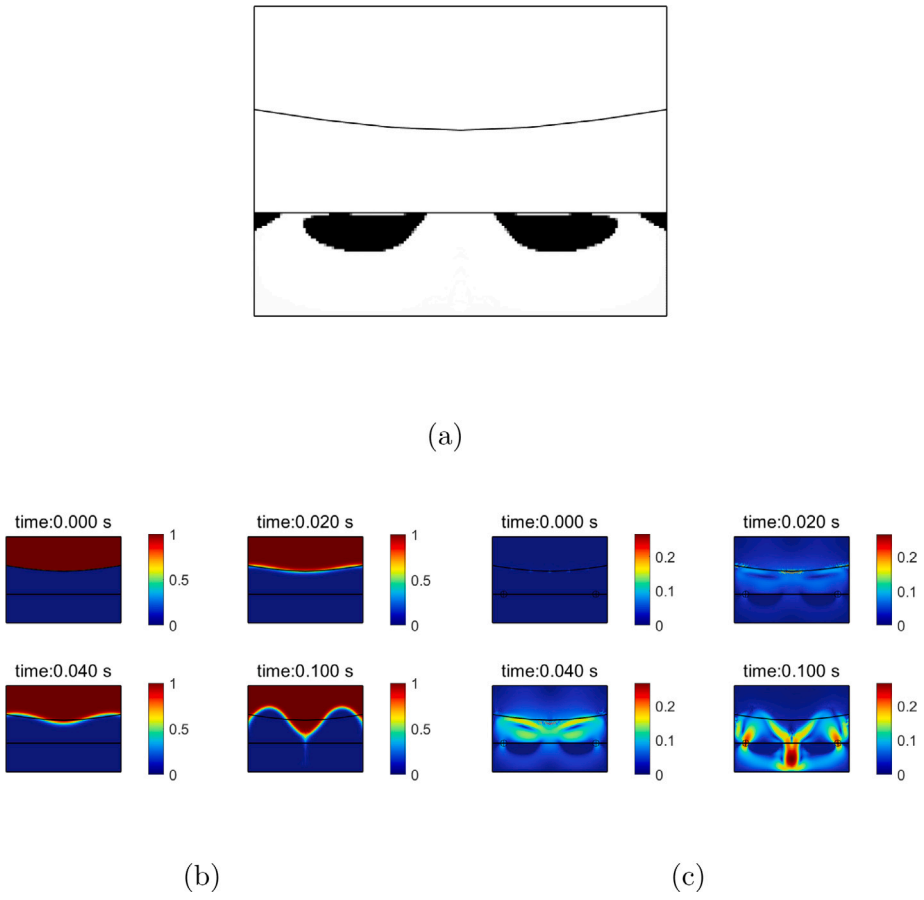

Fig. 9. (a) an optimized result ($x_1 = 0.002$ m, $x_2 = 0.008$ m, $y_1 = y_2 = 0.0150$ m, $\sigma = 2.5\times10^{-4}$), (b) and (c) the phase plot and the corresponding fluid velocity.

and 7(a). This Rayleigh–Taylor instability is widely observed from daily life, i.e., milk or ink drop above water, to gigantic natural phenomena such as volcanic eruption, numerical explosion and supernova explosion. This interesting phenomenon starts from the formulation of small perturbation amplitudes which allows us to obtain the linearized governing equation [1]. This also generates the sinusoidal shaped-surface and then causes exponential instability growth as follows:.

$$\begin{aligned}\xi &= \xi_0 \cosh(\gamma t) + \frac{\dot{\xi}_0}{\gamma}\sinh(\gamma t)\\ \gamma &= \sqrt{A_T k g - \frac{\sigma k^3}{\rho_2+\rho_1}}, A_T = \frac{\rho_2-\rho_1}{\rho_2+\rho_1}\end{aligned} \tag{24}$$

where the perturbation height and the initial perturbation height are denoted by ξ and ξ_0 and the initial velocity is denoted by $\dot{\xi}_0$. The wavenumber of the initial shape of fluid is denoted by k. In this linearized formulation, it can be known that the initial fluid motion is mainly dominated by the densities of fluids and the surface tension coefficient and importantly is not related to the fluid above; in fact, the effect of the fluid above is small and not reflected in this linearized equation. The consideration of this phenomenon in topology optimization is challenging as the joint or separation of fluid during the breakup and merging of two phase domains should be considered and the contact to solid surface should be considered too from not only a simulation point of view but also an optimization point of view.

To simulate and optimize this phenomenon, this research considers the topology optimization problem in Fig. 7(b). With the initially set sinusoidal shaped water, water will drop obeying the Rayleigh–Taylor instability. Then by the developed topology optimization, it is intended to design a bottom structure in order to detuor the dropping fluid and concentrate the fluid dynamic energy to specified areas. For the topology optimization with two-phase fluid, it is one of the challenging aspects that the fluid phase should be fixed in the pseudo-rigid domain. In other words, the design domain modeled as the pseudo-rigid domain should not be fluid and therefore, the fluid velocities should be modeled as zeros. From an optimization point of view, it is difficult to obtain numerically stable solutions and capture this singularity with a fixed time step. In addition to this, it is also found that the form of the objective function can be modified in the form with the circle domains defined by the centers and the distribution parameters. With the integration of fluid velocity at the circle domain, the objective function becomes suddenly vanish at the outsides of the

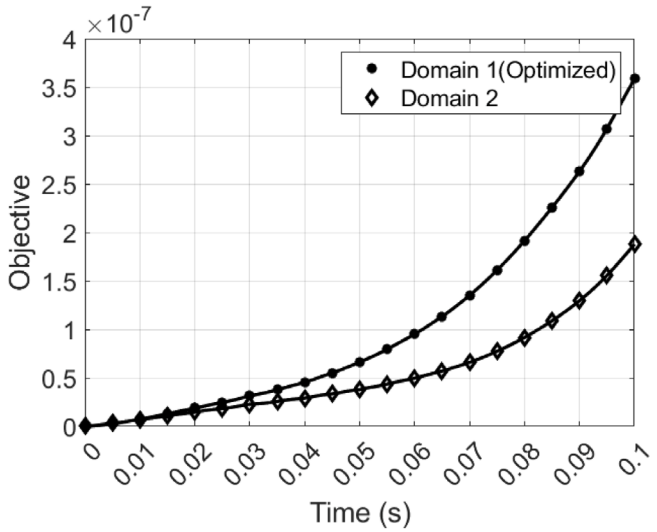

(a)

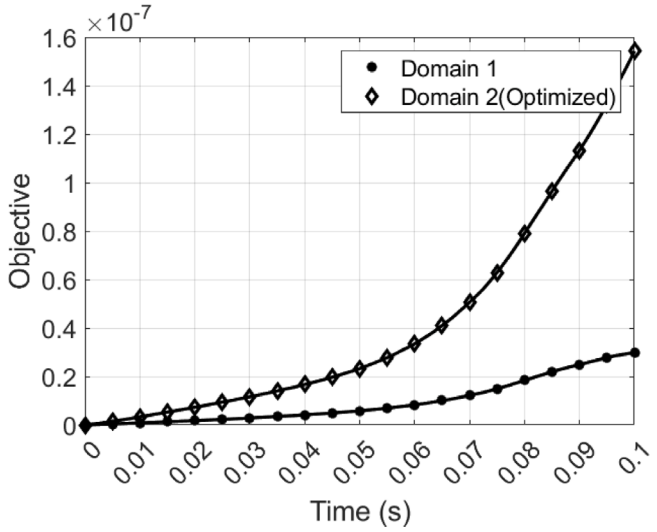

Fig. 10. (a) Response comparison of Fig. 8 and (b) response comparison of Fig. 9. (Domain 1: Objective domain 1 with $x_1 = 0.002$ m, $x_2 = 0.008$ m, $y_1 = y_2 = 0.011$ m, Domain 2: Objective domain 2 with $x_1 = 0.002$ m, $x_2 = 0.008$ m, $y_1 = y_2 = 0.050$ m).

objective domains that can be the sources of the discontinuous sources at the adjoint equations. After considering all, the following objective functions embedding the functions similar to the normal distributions.

$$\psi_1 = e^{\left(-\frac{1}{2}\left(\left(\frac{x-x_c^1}{\sigma}\right)^2+\left(\frac{y-y_c^1}{\sigma}\right)^2\right)\right)}, \psi_2 = e^{\left(-\frac{1}{2}\left(\left(\frac{x-x_c^2}{\sigma}\right)^2+\left(\frac{y-y_c^2}{\sigma}\right)^2\right)\right)} \tag{25}$$

where the standard deviation is denoted by σ and the centers of the distributions are denoted by (x_c^1, y_c^1) and (x_c^2, y_c^2). The benefit of the above function is that the source terms of the adjoint equation become smoothly changed and it can help the convergence of the adjoint solver and varying the value of the σ, the area of consideration can be indirectly controlled. With the above functions, the objective function with the norm of the velocity is defined as follows:

$$J = -\int_{0_\Omega} |\mathbf{u}|_{t=t_f} \times (\psi_1 + \psi_2) \mathrm{d}\Omega \tag{26}$$

With this, it is beneficial to change the normal distribution parameters to enlarge or small the effective areas of the objective domain.

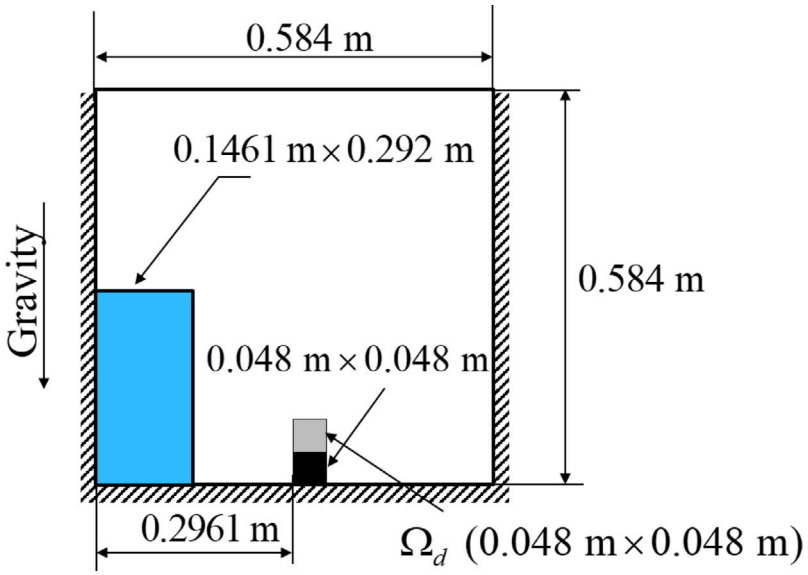

Fig. 11. Dam breaking example ($\mu_1 = 1$ Pa s $\mu_2 = 1$ Pa s, $\rho_1 = 1$ kg/m^3, $\rho_2 = 1000$ kg/m^3, $\sigma =$ 0.07 N/m, Simulation time: 0.3 s, time increment: 0.01 s).

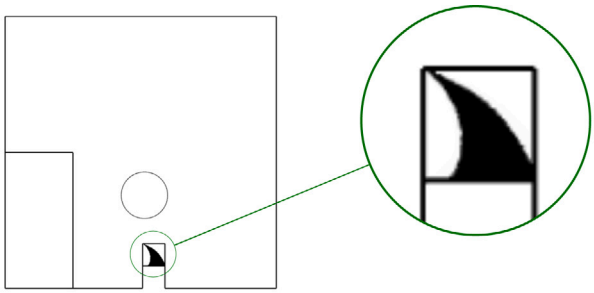

(a)

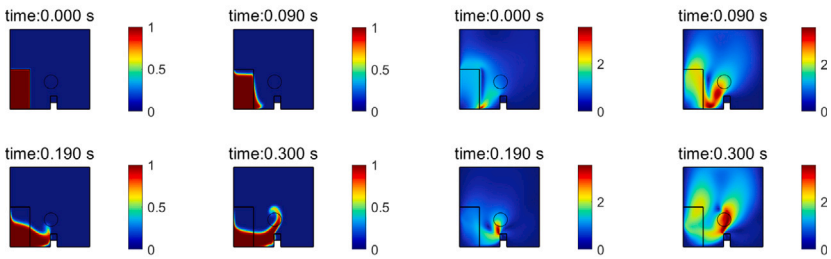

(b) (c)

Fig. 12. (a) An optimized result (Objective domain: 0.05 m radius circle at (0.3 m,0.2 m)), (b) and (c) the phase plot and the corresponding fluid velocity.

Fig. 8(a) shows the optimized layout with the parameters. The objective of this problem is to maximize the fluid velocity at the target domain at 0.1 s. To obtain this design, the symmetricity condition is imposed along the center line as an asymmetric design can be obtained due to the nonlinear solver in fluid. Several structures are distributed and no structure appear near to the

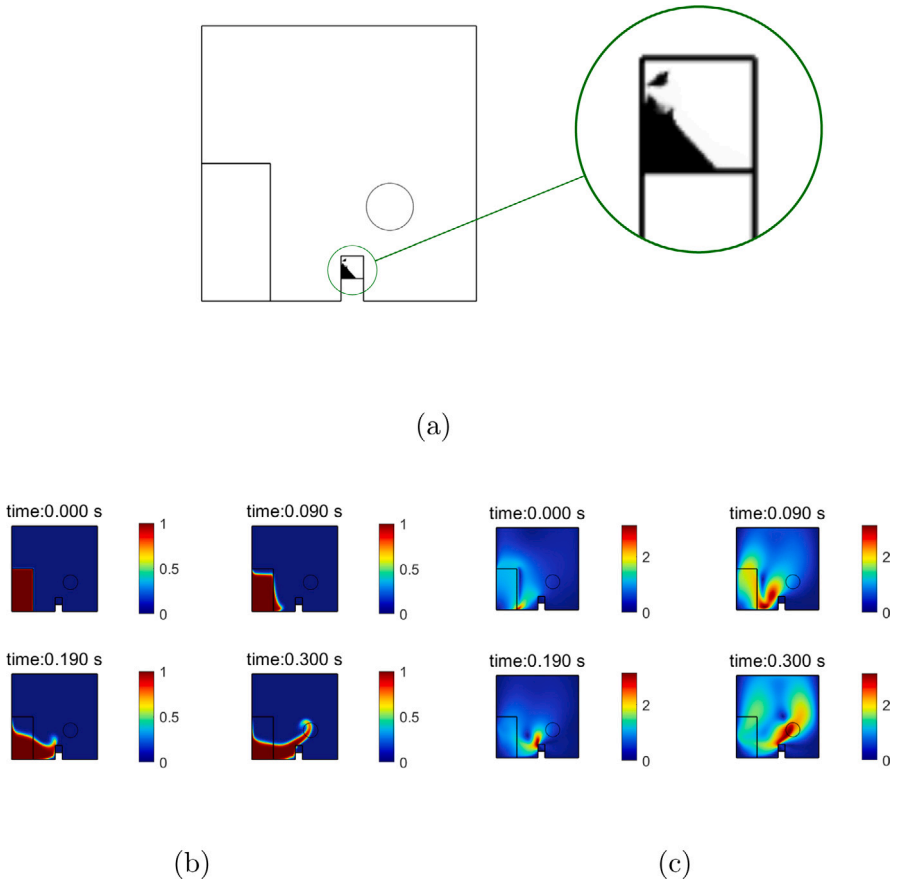

Fig. 13. (a) An optimized result (Objective domain: 0.05 m radius circle at (0.4 m,0.2 m)), (b) and (c) the phase plot and the corresponding fluid velocity.

objective domain. And the small structure appear at the bottom line. Fig. 8(b) shows the motion of the level-set variable. The domain rendered with red color is water and the domain rendered with blue color is air. At 0 s, the non-zero fluid velocity near the interface boundary is observed. At 0.025 s, the water is dropping and the slight motion of the water causes the motion of air (Fig. 8(c)). At 0.05 s, water drops further down and the air motion is circulating and it maximizes the air motion at the target domains. Due to the complex motions of air flow, some oscillations in the objective function exist.

Fig. 9(a) shows an optimized layout with the different objective domain. The center is moved. As in the first example, it is intended to find out an optimized layout moving air and maximizing the air velocity caused by the two fluid interaction at 0.1 s. Fig. 9(b) and (c) show the levelset value and the air velocity. The investigation of these plots reveals that the design concentrates the air velocity at the designated domain successfully (see Fig. 10).

3.3. Example 3: Dam-break problem

For the next example, the dam-break problem is considered in Fig. 11. After the dam breaks, water at the left side flows to the right side while the right small rectangular box blocks the fluid motion causing some stochastic movements of fluid. In this example, it is aimed to control the fluid motion by the present topology optimization scheme. The optimization formulation with the fluid velocity objective and the less-than constraint condition is set as follows:

$$\begin{aligned} &\underset{\gamma}{\text{Min}} \quad J = -\int_{0_\Omega} |\mathbf{u} \times \phi|_{i=t_f} \, \mathrm{d}\Omega \\ &\text{Subject to} \sum_{e=1}^{N_e} \gamma_e \mathrm{v}_e \leq \mathrm{mass}_0 \\ &\gamma = [\gamma_1, \gamma_2, \ldots, \gamma_{N_e}], \quad \gamma_{\min} \leqslant \gamma \leqslant 1, \quad \gamma_{\min} = 0.001 \end{aligned} \tag{27}$$

For the simulation, the time simulation and the time increment are set to 0.3 s and 0.01 s,respectively. In this optimization, the circular objective domain is considered and moved for the present numerical examples.

For the first optimization, the circular objective domain marked in Fig. 12(a) is set and the fin-shape optimized layout in Fig. 12 can be obtained. By blocking the fluid motion, the fluid can be directed toward the objective domain. Note that the fluid motion

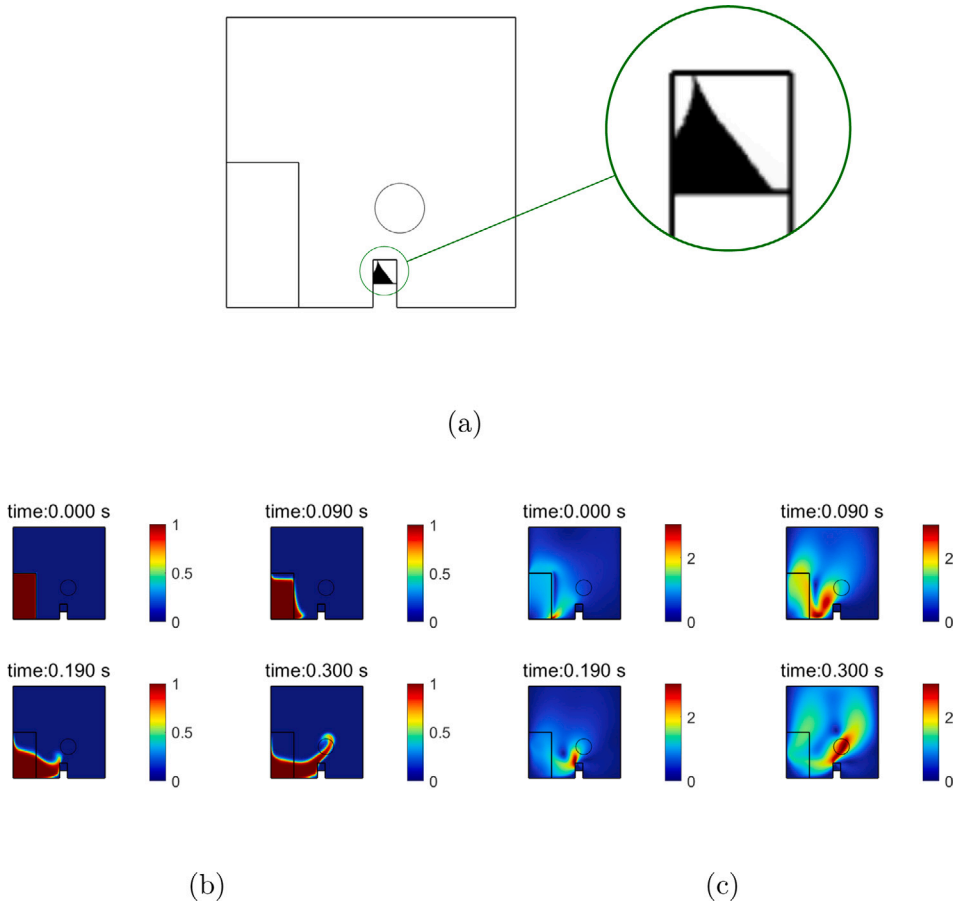

Fig. 14. (a) an optimized result (Objective domain: 0.05 m radius circle at (0.35,0.2)), (b) and (c) the phase plot and the corresponding fluid velocity.

toward the right side is effectively blocked by the fin-shape optimized layout. Fig. 12(b) and (c) show the fluid motion at some represent times. By changing the position of the objective domain, it is possible to obtain some different layouts. In Figs. 13 and 14, some different designs with the different objective domains are presented. This example also suggests that the present scheme can be applied for topology optimization with two-phase fluid.

4. Conclusions

A novel two-phase fluid topology optimization scheme is devised, wherein the laminar Navier–Stokes equation and the levelset function for two-phase fluid simulation are seamlessly integrated using the VOF approach. The adjoint sensitivity is derived employing the calculus of variation and subsequently incorporated into the finite element method framework. Additionally, to accurately capture the evolution of the interfacing, the model takes into account the surface tension phenomenon between the fluids. Based on the results of the presented examples, the followings are found. First of all, this research reveals that the fluid topology optimization finding out the pseudo-rigid domain is possible to control the smooth motion of two-phase fluids. By optimizing the pseudo-rigid domain, the transient motions of fluids can be controlled. Secondly, depending on the fluid motion and the simulation conditions, the nature of the present topology optimization formulation becomes different compared with the structure topology optimization. This characteristics can be found by investigating the form of the mass constraint which is merely introduced to enhance the convergence of the optimization process. When the fluid resistance has a positive effect to the objective function, it is better to use solid as much as possible and the less-than mass constraint is considered. On the other hand, the larger-than mass constraint can be considered. Thirdly, the transient or stochastic motion of multi-phase fluid necessitates meticulous consideration from the perspective of topology optimization. This arises from the fact that minor disparities in initial conditions, such as the initial fluid velocity, initial fluid distribution, and simulation conditions, can lead to substantial divergences in the final outcomes. Consequently, doubts arise concerning the feasibility of achieving a sufficiently smooth response that encompasses fluid behaviors capable of providing the smooth sensitivity required for optimization. In short, the present study develops a new optimization scheme considering two-phase fluid. One limitation of this research is that the numerical difficulties of two-phase fluid simulation prevent consideration of complex-shaped interfaces between two fluids. In future research, the present study can be extended for the mixing device. The extension to 3 dimensional problem is also possible.

Declaration of competing interest

The authors declare that they have no known competing financial interests or personal relationships that could have appeared to influence the work reported in this paper.

Funding information

This work was supported by a National Research Foundation of Korea (NRF) grant funded by the Korean government (MSIT) (NRF-2019R1A2C2084974).

Data availability

Data will be made available on request.

References

[1] H. Kull, Theory of the Rayleigh-Taylor instability, Phys. Rep. 206 (5) (1991) 197–325, http://dx.doi.org/10.1016/0370-1573(91)90153-D.
[2] I. Khan, M. Wang, Y. Zhang, W. Tian, G. Su, S. Qiu, Two-phase bubbly flow simulation using CFD method: A review of models for interfacial forces, Prog. Nucl. Energy 125 (2020) 103360, http://dx.doi.org/10.1016/j.pnucene.2020.103360.
[3] S.A. Khana, A. Shahb, Simulation of the two-dimensional Rayleigh-Taylor instability problem by using diffuse-interface model, AIP Adv. 9 (085312) (2022).
[4] S. Tiwari, J. Kuhnert, Modeling of two-phase flows with surface tension by finite pointset method (FPM), J. Comput. Appl. Math. 203 (2) (2007) 376–386, http://dx.doi.org/10.1016/j.cam.2006.04.048, Special Issue: The first Indo-German Conference on PDE, Scientific Computing and Optimization in Applications.
[5] J. Brackbill, D. Kothe, C. Zemach, A continuum method for modeling surface tension, J. Comput. Phys. 100 (2) (1992) 335–354, http://dx.doi.org/10.1016/0021-9991(92)90240-Y.
[6] T. Borrvall, J. Petersson, Topology optimization of fluids in Stokes flow, Internat. J. Numer. Methods Fluids (2003) 77–107.
[7] C.M. Okubo, L.F. Sá, C.Y. Kiyono, E.C. Silva, A discrete adjoint approach based on finite differences applied to topology optimization of flow problems, Comput. Methods Appl. Mech. Engrg. 389 (2022) 114406, http://dx.doi.org/10.1016/j.cma.2021.114406.
[8] J. Yan, R. Xiang, D. Kamensky, M.T. Tolley, J.T. Hwang, Topology optimization with automated derivative computation for multidisciplinary design problems, Struct. Multidisc. Optim. 65 (2022) 114406.
[9] G.H. Yoon, Transient sensitivity analysis and topology optimization for particle motion in steady state laminar fluid, Comput. Methods Appl. Mech. Engrg. 367 (2020) 113096.
[10] Y. Deng, Z. Liu, P. Zhang, Y. Liu, Y. Wu, Topology optimization of unsteady incompressible Navier-Stokes flows, J. Comput. Phys. 230 (2011) 6688–6708.
[11] S. Kreissl, G. Pingen, K. Maute, Topology optimization for unsteady flow, Internat. J. Numer. Methods Engrg. 87 (2011) 1229–1253.
[12] A. Ghasemi, A. Elham, Efficient multi-stage aerodynamic topology optimization using an operator-based analytical differentiation, Struct. Multidisc. Optim. 65 (130) (2022).
[13] G.H. Yoon, Topological design of heat dissipating structure with forced convective heat transfer, J. Mech. Sci. Technol. 24 (6) (2010) 1225–1233.
[14] E. Dede, Multiphysics topology optimization of heat transfer and fluid flow systems, in: Proceedings of the COMSOL Conference, COMSOL Conference, 2009.
[15] H. Li, T. Kondoh, P. Jolivet, K. Furuta, T. Yamada, B. Zhu, K. Izui, S. Nishiwaki, Three-dimensional topology optimization of a fluid–structure system using body-fitted mesh adaption based on the level-set method, Appl. Math. Model. 101 (2022) 276–308.
[16] X. Qian, E.M. Dede, Topology optimization of a coupled thermal-fluid system under a tangential thermal gradient constraint, Struct. Multidiscip. Optim. 54 (3) (2016) 531–551.
[17] A. Iga, S. Nishiwaki, K. Izui, M. Yoshimura, Topology optimization for thermal conductors considering design-dependent effects, including heat conduction and convection, Int. J. Heat Mass Transfer 52 (2009) 2721–2732.
[18] Y. Joo, I. Lee, S. Kim, Efficient three-dimensional topology optimization of heat sinks in natural convection using the shape-dependent convection model, Int. J. Heat Mass Transfer 127 (2018) 23–40.
[19] F. Dugast, Y. Favennec, C. Josset, Y. Fan, L. Luo, Topology optimization of thermal fluid flows with an adjoint lattice Boltzmann method, J. Comput. Phys. 365 (2018) 376–404.
[20] J. Alexandersen, N. Aage, C.S. Andreasen, O. Sigmund, Topology optimisation for natural convection problems, Internat. J. Numer. Methods Fluids 76 (10) (2012) 699–721.
[21] Z. Duan, G. Xie, X. Li, Topology optimization design of scramjet structures with forced convective heat transfer on unstructured meshes, J. Therm. Sci. Eng. Appl. 15 (1) (2022) 011011, http://dx.doi.org/10.1115/1.4055608, arXiv:https://asmedigitalcollection.asme.org/thermalscienceapplication/article-pdf/15/1/011011/6927430/tsea_15_1_011011.pdf.
[22] R. Picelli, E. Moscatelli, P.V.M. Yamabe, D.H. Alonso, S. Ranjbarzadeh, R. dos Santos Gioria, J.R. Meneghini, E.C.N. Silva, Topology optimization of turbulent fluid flow via the TOBS method and a geometry trimming procedure, Struct. Multidisc. Optim. 65 (34) (2022).
[23] A. Gersborg-Hansen, O. Sigmund, R. Haber, Topology optimization of channel flow problems, Struct. Multidiscip. Optim. 30 (2005) 181–192.
[24] L.C. Høghøj, D.R. Nørhave, J. Alexandersen, O. Sigmund, C.S. Andreasen, Topology optimization of two fluid heat exchangers, Int. J. Heat Mass Transfer 163 (2020) 120543.
[25] G. Anjos, N. Borhani, N. Mangiavacchi, J. Thome, A 3D moving mesh finite element method for two-phase flows, J. Comput. Phys. 270 (2014) 366–377, http://dx.doi.org/10.1016/j.jcp.2014.03.067.
[26] J. Hua, D. Mortensen, A front tracking method for simulation of two-phase interfacial flows on adaptive unstructured meshes for complex geometries, Int. J. Multiph. Flow. 119 (2019) 166–179.
[27] X. Liu, B. Zhang, J. Sun, An improved implicit re-initialization method for the level set function applied to shape and topology optimization of fluid, J. Comput. Appl. Math. 281 (2015) 207–229, http://dx.doi.org/10.1016/j.cam.2014.12.017.
[28] E. Olsson, G. Kreiss, S. Zahedi, A conservative level set method for two phase flow II, J. Comput. Phys. 225 (2007) 785–807.
[29] C. Bernardi, S. Maarouf, D. Yakoubi, Finite element discretization of two immiscible fluids with surface tension, 2015, hal-01128264.
[30] R. Courant, K. Friedrichs, H. Lewy, Über die partiellen, Über die partiellen differenzengleichungen der mathematischen physik, Phys. Math. Ann. 100 (1928) 32–74.
[31] Y. Deng, Z. Liu, P. Zhang, Y. Liu, Y. Wu, Topology optimization of unsteady incompressible Navier–Stokes flows, J. Comput. Phys. 230 (17) (2011) 6688–6708.
[32] K. Svanberg, The method of moving asymptotes – a new method for structural optimization, Internat. J. Numer. Methods Engrg. 24 (2) (1987) 359–373.